Supplementary Information：

Sulfur-Doped Wood-derived Porous Carbon for Optimizing Electromagnetic Response Performance

Haihua Hu,[a] Yixing Li,[a,]* Tong Gao,[a] Siyu Yan,[a] Shiting Wu,[b] Sateesh Bandaru,[b] Yun Zheng,[a] Gaowu Qin[a] and Xuefeng Zhang[a, b,]*

[a] Key Laboratory for Anisotropy and Texture of Materials (MOE), School of Materials Science and Engineering, Northeastern University, Shenyang 110819, P. R. China

[b] Institute of Advanced Magnetic Materials, College of Materials & Environmental Engineering, Hangzhou Dianzi University, Hangzhou 310012, P. R. China

* Corresponding authors.

E-mail addresses: zhangxf@atm.neu.edu.cn (X. F. Zhang), liyx@mail.neu.edu.cn (Y.X. Li)

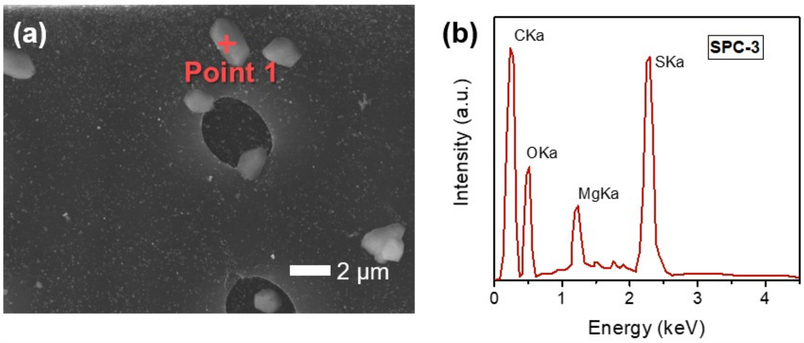

(c) Element	Mass%	Atom%
C	57.50	68.6
O	26.65	23.87
Mg	3.13	1.85
S	12.72	5.68
Total	100	100

Fig. S1 The EDS elemental point-scanned of the nanoparticles for the SPC-3 sample. (a) The SEM image; (b) Spectrum; (c) The table of the contents of elements.

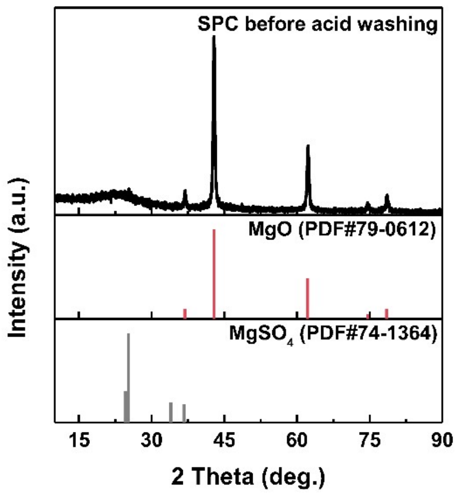

Fig. S2 XRD patterns of SPC samples before acid washing.

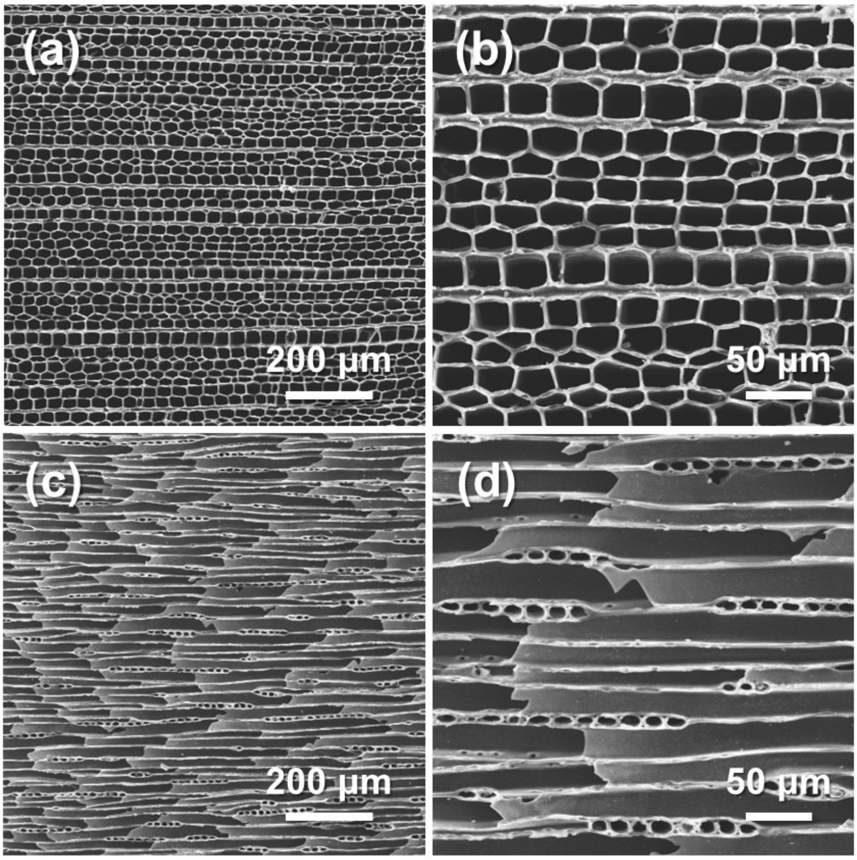

Fig. S3 Microstructure characterization of PC.

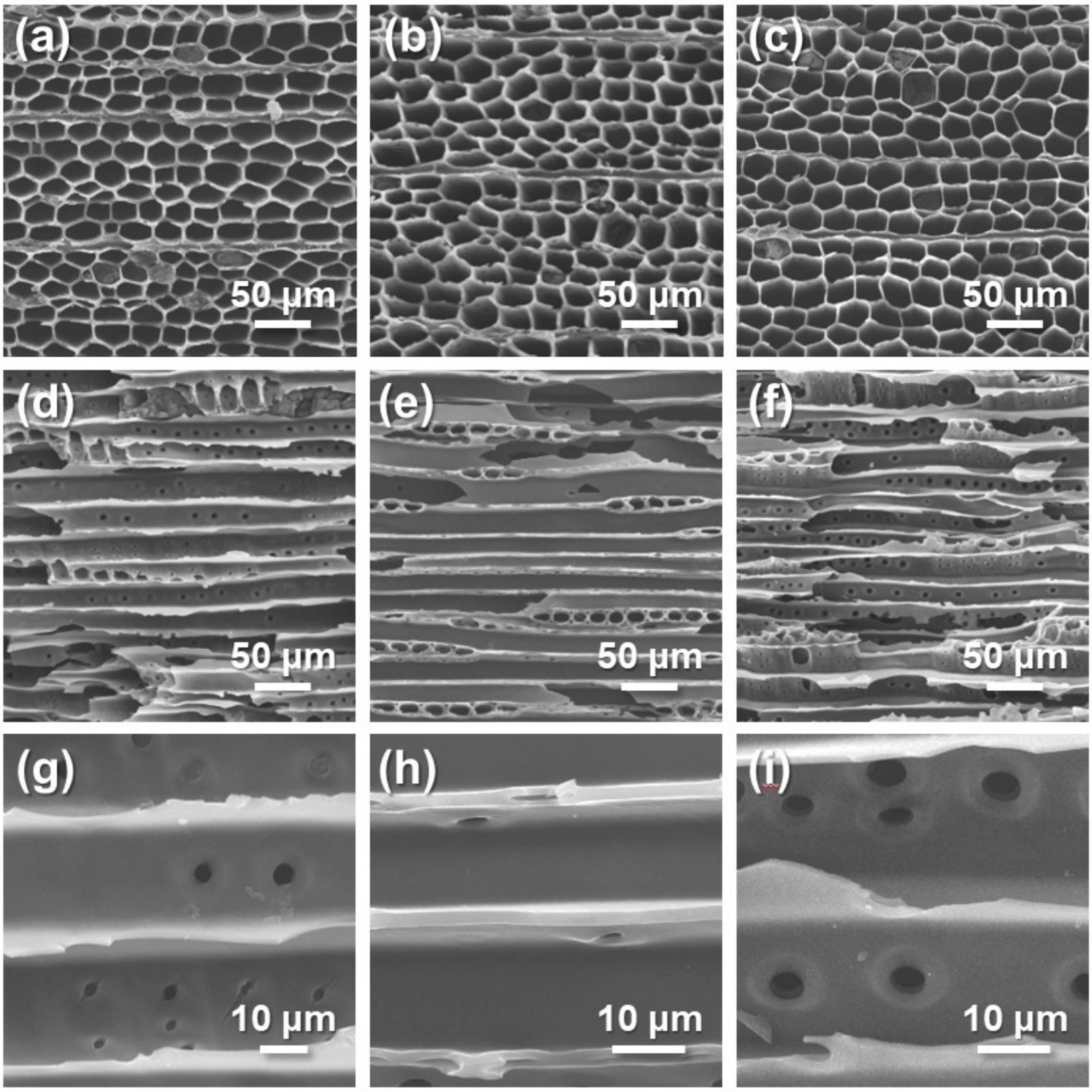

Fig. S4 Microstructure characterization of (a), (d), (g) SPC-1, (b), (e), (h) SPC-2 and (c), (f), (i) SPC-3.

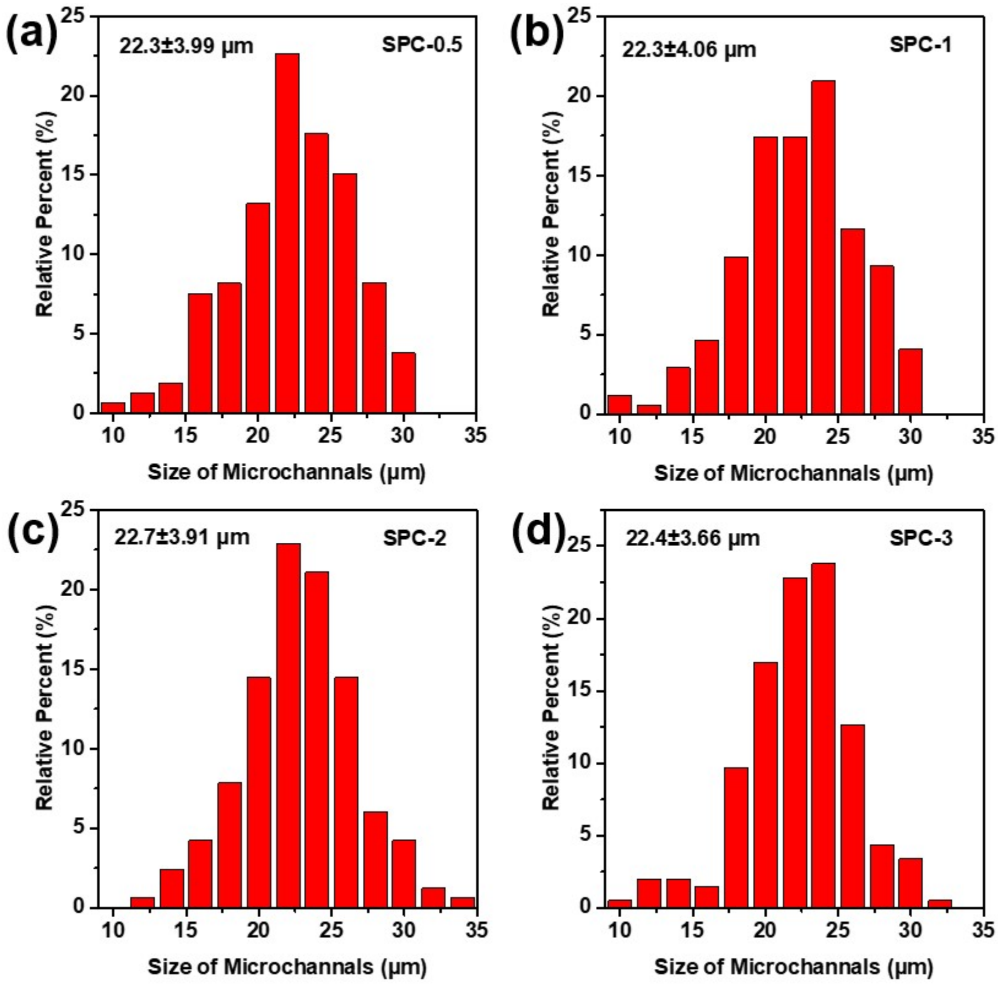

Fig. S5 Dimension statistical graph of microchannels in (a) SPC-0.5, (b) SPC-1, (c) SPC-2 and (d) SPC-3.

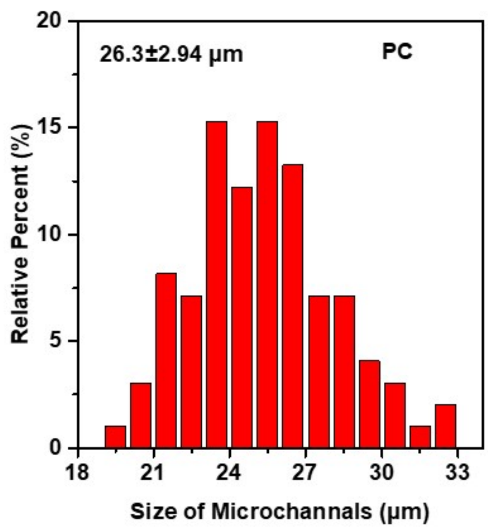

Fig. S6 Dimension statistical graph of microchannels for the PC sample.

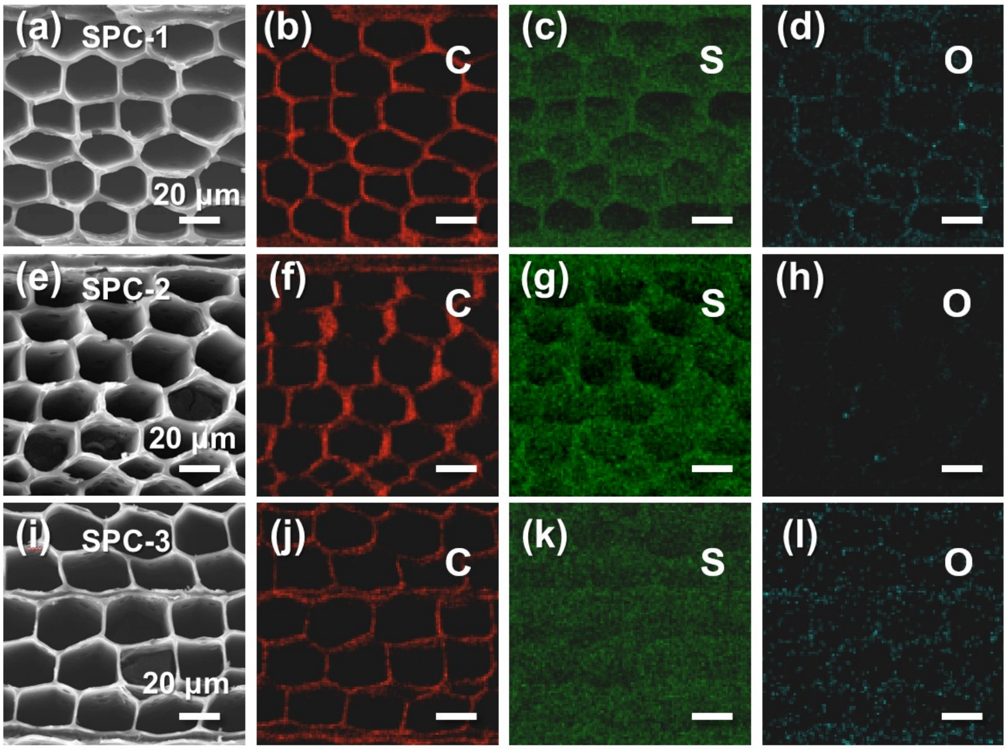

Fig. S7 Microstructure characterization of SPC-1, SPC-2, and SPC-3, and elemental-mapping images of C, S, and O, respectively.

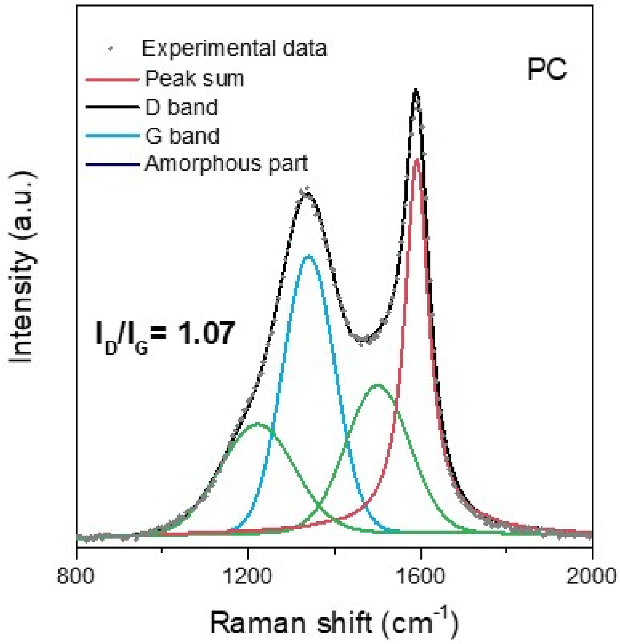

Fig. S8 Raman spectrum of the PC sample.

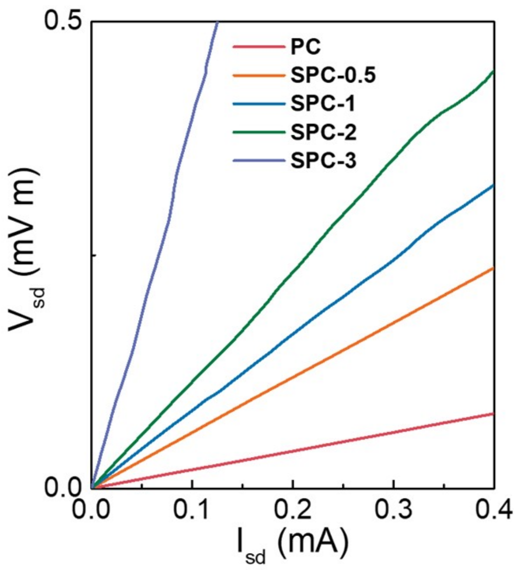

Fig. S9 The I-V curves for PC and SPC samples.

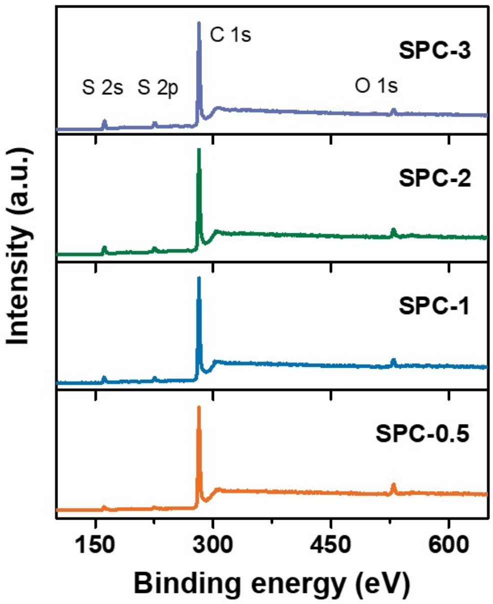

Fig. S10 X-ray photoelectron spectroscopy for SPC-0.5, 1, 2 and 3.

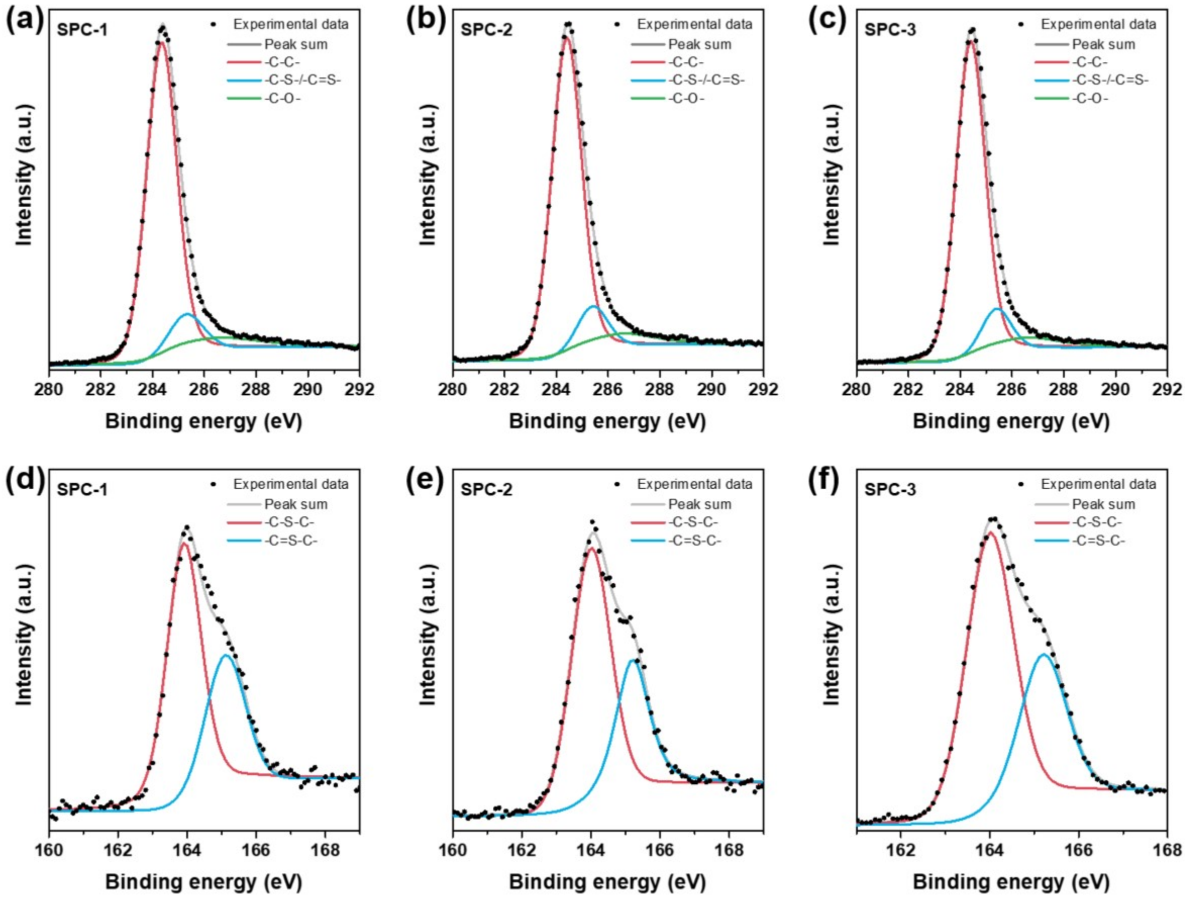

Fig. S11 XPS spectra of C_{1s} a-c and S_{2p} d-f peaks for SPC-1, 2, 3 samples.

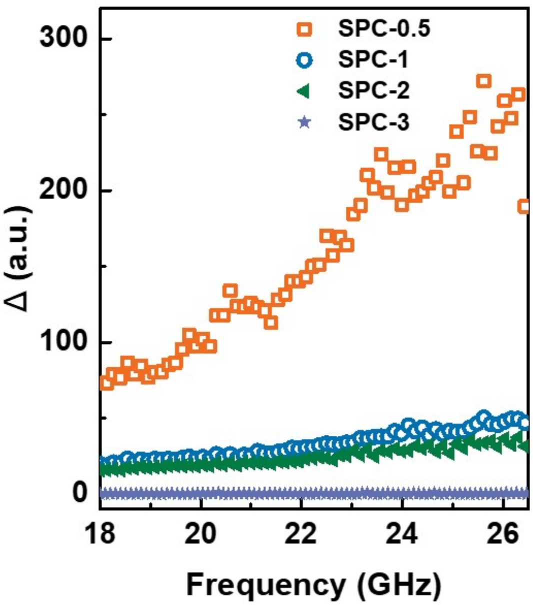

Fig. S12 Impedance matching degree (*Δ*) dependent of frequency of SPC-0.5, SPC-1, SPC- 2 and SPC- 3 with the thickness of 2 mm.

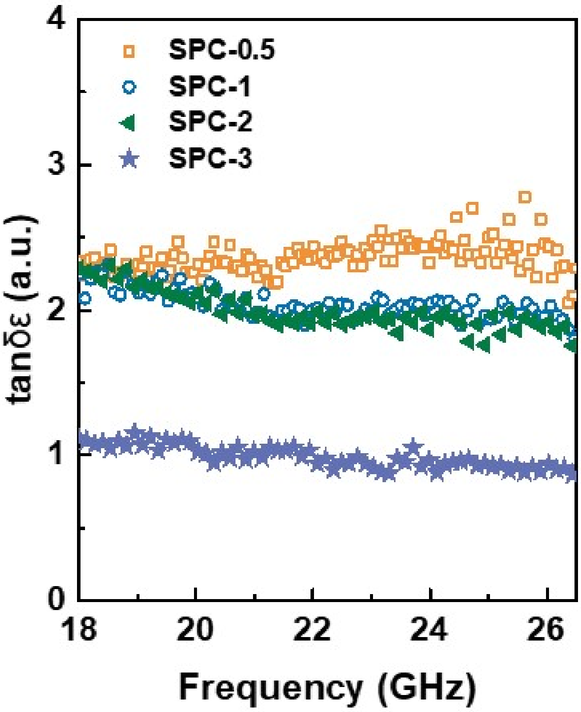

Fig. S13 The dielectric loss tangent (tan δε) of SPC samples.

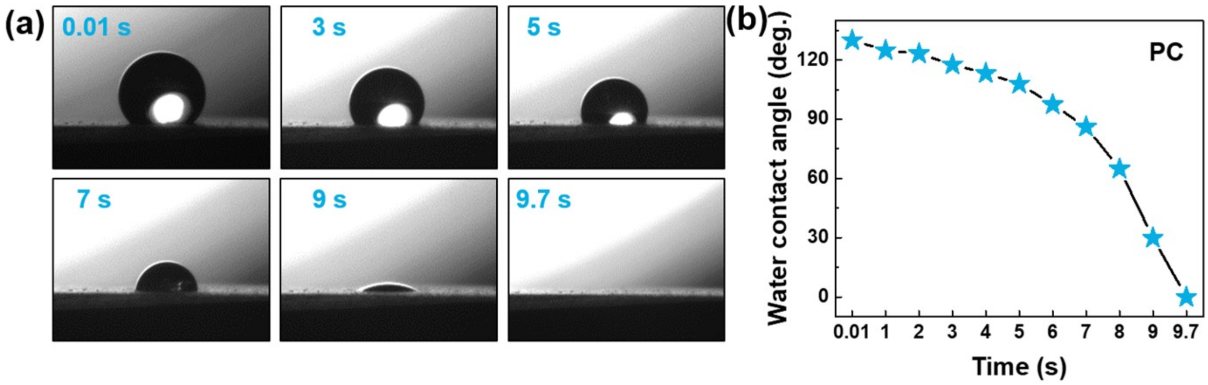

Fig. S14 (a) The wetting behavior of the water droplet on the surface of the PC and (b) the change of water contact angles during the wetting behavior test.

Table S1 Contents of Elements including C, S and O for SPC-0.5, SPC-1, SPC-2 and SPC-3.

Sample	Carbon (at. %)	Sulfur (at. %)	Oxygen (at. %)
SPC-0.5	95.11	2.86	2.03
SPC-1	93.42	3.77	2.81
SPC-2	92.98	5.29	1.73
SPC-3	91.47	8.33	0.2

Table S2 The microwave absorption performance of PC and SPC samples compared with other reported carbon-based materials.

Sample	Thickness (mm)	RL_{min} (dB)	Effective bandwidth (GHz)	Ref.
Graphene@Fe	2.0	-27	4.25	S1
Graphene@Fe_3O_4@SiO_2@NiO	3.0	-27	4.8	S2
3D graphene-Fe_3O_4	3.0	-22.5	4.8	S3
RGO/$MnFe_2O_4$	3.0	-29	5	S4
N-rGA/Ni	2.4	-27	6.7	S5
$CoFe_2O_4$/C/PANI	2.5	-33.6	8.8	S6
ZnO/Carbon foam	2.35	-35.7	2.75	S7
N-doped porous carbon foam	2	-46	5.4	S8
Fe_3O_4/CF	2.5	-27	5.2	S9
Cobalt/helical carbon fiber	2.0	-30	6.2	S10
Accordion-like Ni@C	1.8	-86.9	6.6	S11
Nickel/Porous Carbon	1.8	-28.4	4.5	S12
Cobalt/H-Porous carbon	2.4	-21	6.2	S13
Nickel/H-Porous carbon	2.5	-19	8.3	S13
Mo_2C/ Porous carbon	2.21	-45.3	3.96	S14
hierarchically tubular C/Co	2	-52.3	5	S15
ZFC-700	1.5	-30.4	4.96	S16
Fe_3O_4/CNT	2	-26.5	6.8	S17
Fe_2O_3/CNT	1.5	-22	4.8	S18
FeSiAl/CNT	2	-22	4.2	S19
PANI/Fe_3O_4/CNT	4	-17	7.2	S20
PC	**1.92**	**-19.76**	**5.01**	**This work**
SPC-2	**1.91**	**-32.76**	**6.4**	**This work**

Table S3 The proportions of SE_A and SE_R in the total SE value.

Sample	SE_R (dB)	SE_R/SE (%)	SE_A (dB)	SE_A/SE (%)
SPC (Original)	1.43	31.9	6.6	68.1
SPC-10 min	1.71	34.9	9.7	65.1
SPC-15 min	2.1	39.7	12.4	60.3
SPC-20 min	2.53	43.5	17.8	56.5
SPC-25 min	3.2	51.9	26.5	48.0
SPC-30 min	3.4	54.3	27.5	45.7

References

S1 X. Zhao, Z. Zhang, L. Wang, K. Xi, Q. Cao, D. Wang, Y. Yang and Y. Du, *Sci. Rep.*, 2013, **3**, 3421.

S2 L. Wang, Y. Huang, X. Sun, H. Huang, P. Liu , M. Zong and Y. Wang, *Nanoscale*, 2014, **6**, 3157-3164.

S3 C. Hu, Z. Mou, G. Lu, N. Chen, Z. Dong , M. Hu and L. Qu, *Phys. Chem. Chem. Phys.*, 2013, **15**, 13038-13043.

S4 X. J. Zhang, G. S. Wang, W. Q. Cao, Y. Z. Wei, J. F. Liang , L. Guo and M.-S. Cao, *ACS Appl. Mater. Interfaces*, 2014, **6**, 7471-7478.

S5 J. Tang, N. Liang, L. Wang, J. Li, G. Tian , D. Zhang, S. Feng and H. Yue, *Carbon*, 2019, **152**, 575-586.

S6 T. Hou, Z. Jia, A. Feng, Z. Zhou, X. Liu , H. Lv and G. Wu, *J. Mater. Sci. Tech.*, 2020, **68**, 61-69.

S7 X. Liang, B. Quan, Z. Man, B. Cao, N. Li C. Wang, G. Ji and T. Yu, *ACS Appl. Mater. Interfaces*, 2019, **11**, 30228-30233.

S8 J. Yan, Y. Huang, C. Chen, X. Liu and H. Liu, *Carbon*, 2019, **152**, 545-555.

S9 Y. Liu, Z. Chen, W. Xie, S. Song, Y. Zhang and L. Dong, *ACS Sustain. Chem. Eng.*, 2019, **7**, 5318-5328.

S10 F. Wu, K. Yang, Q. Li, T. Shah, M. Ahmad , Q. Zhang and B. Zhang, *Carbon*, 2021, **173**, 918-931.

S11 Z. Xiang, C. Huang, Y. Song, B. Deng, X. Zhang X. Zhu, D. Batalu, O. Tutunaru and W. Lu, *Carbon*, 2020, **167**, 364-377.

S12 S. Qiu, H. Lyu, J. Liu, Y. Liu, N. Wu and W. Liu, *ACS Appl. Mater. Interfaces*, 2016, **8**, 20258-20266.

S13 T. Huang, Z. Wu, Q. Yu, D. Tan and L. Li, *Chem. Eng. J.*, 2019, **359**, 69-78.

S14 S. Dai, Y. Cheng, B. Quan, X. Liang, W. Liu, Z. Yang, G. Ji and Y. Du, *Nanoscale*, 2018, **10**, 6945-6953.

S15 Z. Wu, K. Pei, L. Xing, X. Yu, W. You and R. Che, *Adv. Funct. Mater.*, 2019, **29**, 1901448.

S16 W. Liu, L. Liu, G. Ji, D. Li, Y. Zhang J. Ma and Y. Du, *ACS Sustain. Chem. Eng.*, 2017, **5**, 7961-7971.

S17 N. Li, G. W. Huang, Y. Q. Li, H. M. Xiao, Q. P. Feng , N. Hu and S.-Y. Fu, *ACS Appl. Mater. Interfaces*, 2017, **9**, 2973-2983.

S18 L. Wang, X. Yu, X. Li, J. Zhang, M. Wang and R. Che, *Carbon*, 2019, **155**, 298-308.

S19 L. Huang, X. Liu, D. Chuai, Y. Chen and R. Yu, *Sci. Rep.*, 2016, **6**, 1-12.

S20 M. S. Cao, J. Yang, W. L. Song, D. Q. Zhang, B. Wen H.-B. Jin, Z.-L. Hou and J. Yuan, *ACS Appl. Mater. Interfaces*, 2012, **4**, 6949-6956.